

Title:

FULL APERTURE BACKSCATTER STATION IMAGER , (FABSI)
DIAGNOSTICS SYSTEM FOR FAR-FIELD IMAGING OF LASER
PLASMA INSTABILITIES ON NOVA.

RECEIVED

JUN 11 1996

OSTI

Author(s):

M. D. WILKE, P-24
J. C. FERNANDEZ, P-24
R. R. BERGGREN, P-24
R. F. HORTON, SAIC, ALBUQUERQUE, NM 87106
D. S. MONTGOMERY, P-24
J. A. FAULKNER, P-24
L. D. LOONEY, P-22
J. R. JIMERSON, P-24

Submitted to:

11th HIGH-TEMPERATURE PLASMA DIAGNOSTICS
CONFERENCE.
MONTEREY, CA
MAY 12-16, 1996

MASTER



Los Alamos
NATIONAL LABORATORY

Los Alamos National Laboratory, an affirmative action/equal opportunity employer, is operated by the University of California for the U.S. Department of Energy under contract W-7405-ENG-36. By acceptance of this article, the publisher recognizes that the U.S. Government retains a nonexclusive, royalty-free license to publish or reproduce the published form of this contribution, or to allow others to do so, for U.S. Government purposes. The Los Alamos National Laboratory requests that the publisher identify this article as work performed under the auspices of the U.S. Department of Energy.

DISTRIBUTION OF THIS DOCUMENT IS UNLIMITED

Form No. 836 R5
ST 2629 10/91

DISCLAIMER

This report was prepared as an account of work sponsored by an agency of the United States Government. Neither the United States Government nor any agency thereof, nor any of their employees, makes any warranty, express or implied, or assumes any legal liability or responsibility for the accuracy, completeness, or usefulness of any information, apparatus, product, or process disclosed, or represents that its use would not infringe privately owned rights. Reference herein to any specific commercial product, process, or service by trade name, trademark, manufacturer, or otherwise does not necessarily constitute or imply its endorsement, recommendation, or favoring by the United States Government or any agency thereof. The views and opinions of authors expressed herein do not necessarily state or reflect those of the United States Government or any agency thereof.

DISCLAIMER

**Portions of this document may be illegible
in electronic image products. Images are
produced from the best available original
document.**

Full aperture backscatter station imager (FABSI) diagnostics system for far-field imaging of laser plasma instabilities on Nova

Mark D. Wilke, Juan C. Fernández, Ralph R. Berggren, Richard F. Horton*, David Montgomery, James Faulkner, Larry Looney and John Jimerson

Los Alamos National Laboratory, Los Alamos, NM 87545

**SAIC, Albuquerque, NM 87106*

(Presented 14 May 1996)

In ICF, the understanding of laser plasma scattering processes is essential for laser target coupling and in controlling the symmetry of indirect drive implosions. The existing Nova Full Aperture Backscatter Station (FABS) has been useful in understanding laser plasma instabilities occurring in hohlraums by measuring the quantity, spectral distribution and near-field spatial distributions of Brillouin and more recently Raman backscatter. Equally important is an understanding of the far-field spatial intensity distribution which provides information on density, temperature and velocity gradient distributions, and which affect capsule implosion symmetry in hohlraums. Such information could potentially help in understanding processes such as filamentation and saturation mechanisms. This paper describes a broad-band, color-corrected far-field imager and associated diagnostics capable of imaging the source of scattered light to better than $25 \mu\text{m}$ resolution. The imager can either image Brillouin or Raman backscatter through the Nova beam 7 focusing lens or be used like a microscope to image side scatter from other beams.

I. INTRODUCTION

The goal of indirect-drive laser inertial confinement fusion (ICF) is to compress a capsule by uniformly irradiating the capsule with x-rays generated from the interaction of high-intensity lasers with the high-Z wall of a confining enclosure called a hohlraum. The understanding of laser-hohlraum interaction is essential to the success of the proposed National Ignition Facility (NIF) where it is hoped to eventually ignite a compressed deuterium-tritium loaded capsule in a hohlraum where plasma electron densities and temperatures are expected to reach $n_e \geq 10^{21} \text{ cm}^{-3}$ and $T_e = 3-5 \text{ keV}$ over scale lengths approaching a centimeter. At present, the proposed wavelength for NIF and the most frequently used wavelength at Nova is $\lambda_l = 351 \text{ nm}$. The laser intensities are on the order of 10^{15} to 10^{16} . For a variety of symmetry issues, Nova hohlraum design has progressed from Au wall only to CH-lined Au walls to the present gas-filled Au hohlraums which mimic current NIF designs¹. Although Nova can not exactly duplicate NIF hohlraum conditions, suitable approximations to portions of the NIF hohlraums have been attempted using toroidal gas-filled hohlraums² and gas bags³. Densities, temperatures, probe-laser intensities and scale lengths approach NIF lengths for shorter periods of time.

The interaction of the high-intensity laser with the plasma contained within these different hohlraums and with the high-Z hohlraum wall can lead to phenomena which often degrade capsule performance through degradation of

implosion symmetry, or by the reduction of laser-hohlraum coupling efficiency. Phenomena include parametric instabilities which produce optical emissions at a variety of optical wavelengths such as stimulated Brillouin scatter (SBS) at $\lambda \sim \lambda_l$, stimulated Raman scatter (SRS) at $\lambda \sim 1\lambda_l$, through $2\lambda_l$, and two-plasmon decay ($2\omega_{pe}$) which leads to emissions at $\lambda \sim 2\lambda_l$, and $\lambda \sim (2/3)\lambda_l$, via secondary processes. Although the instabilities are generally detrimental to capsule performance, characteristics of the resulting scattered light can be used as diagnostics to determine plasma conditions in the interaction region. Because the plasma conditions vary significantly along the path of the laser within the hohlraums, it is possible that in some regions some instabilities will be favored over others or conditions will favor interaction of the instabilities through secondary processes modifying the scattered light. In addition, other plasma phenomena such as light bending from plasma flow⁴ or self-focusing and filamentation⁵ can modify the scattered light either directly or by modification of the plasma conditions.

Near-field spatially averaged scattered light previously measured by FABS⁶ diagnostic is a mix of light determined by a variety of laser-plasma interactions. We have taken the next step to obtain spatially resolved backscatter in the far-field by constructing a FABS imager (FABSI). An early general description of the proposed imager was previously given.⁷ This paper briefly describes FABSI and associated

diagnostics which is near completion and will soon be installed at Nova.

II. OPTICAL SYSTEM

Figure 1 is a schematic of the FABSI optical system. The following is a brief description. A detailed description of the design, fabrication and performance will be the subject of a future paper. Beam-7 1 μm light is reflected by the turning mirror and converted by the KDP crystals to typically 3 ω , 351 nm light which is focused onto the target through a precision fused silica single-element aspheric lens. A random phase plate (RPP) is positioned in the converging beam at a slight angle to the beam between the focusing lens and the target to smooth the beam spot. The converted light which is backscattered from the target passes back through the turning mirror (see transmission curve inset in Fig. 1). The focal length of the Nova focusing lens varies by ~4 cm from 351 nm to 700 nm and produces chromatic aberrations. The RPP introduces wavefront distortion in the backscatter image.

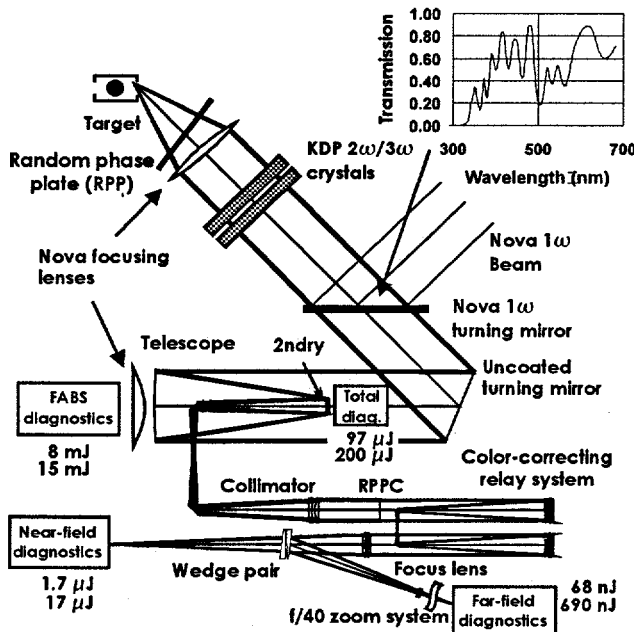


FIG. 1. Schematic of the FABSI optical system and diagnostics.

The backscatter is reflected from a flat located at the original FABS location into a telescope which consists of an uncoated spherical fused-silica primary a multi-element partially transmitting secondary and a tertiary lens. The telescope beam is recollimated to ~30 cm diameter for transmission through the color corrector. An image of the RPP is formed after the recollimator where an RPP compensator (RPPC) is located. The RPPC is etched with a pattern that exactly compensates for the RPP pattern

including distortion from the RPP tilt and converging Nova beam. The future plan to use kinoform phase plates to shape the Nova beam spot requires that the resolution and position accuracy at the RPPC be better than 100 μm referenced at the RPP. Measurements using a CCD camera and tungsten-halide source gave better than 90 μm resolution. Distortion was below measurable levels.

The color corrector consists of two cells each composed of two transmitting and one reflecting element. A beam stop in the color corrector eliminates secondary reflections from tilted crystal surfaces. The beam is then brought to final focus. A wedge set splits the beam sending the majority of the light to a near-field system and the ~4% reflection through a final field lens to the f/10 focus. The beam is further magnified by a telecentric f/10 to f/40 magnifying set of mirrors (not shown) and sent to the far-field imaging diagnostics.

We have measured the resolution at the f/10 and f/40 positions without the RPP/RPPC pair installed to be <20 μm referenced at the target using a tungsten-halide lamp and a CCD imager. We will soon complete testing with the RPP/RPPC pair.

The system can be used either as a backscatter diagnostic for beam 7 or for observing side and near-forward scatter from the other beams. The system also has some capability in locating the source of backscatter longitudinally because of the finite depth of field. Assuming a 20 μm blur, the geometric depth of field is approximately 90 μm for the f/4.3 Nova lens.

III. DIAGNOSTICS

The labeled boxes in Fig. 1 indicate the positions of the various diagnostics packages. The upper (smaller) value near each of the boxes indicates the fraction of SBS which reaches the package, and the lower (larger) value indicates the fraction of SRS assuming that the Nova turning mirror transmission is 0.6 averaged over the SRS spectrum and that the reflection from the first FABSI turning mirror is 4%.

FABS Diagnostics: To prevent having to reconfigure several of the existing FABS diagnostics and data analysis procedures, a subset of the FABS diagnostics is being moved behind the telescope primary. A Nova lens focuses the light onto a diffuser which is viewed by fibers and diodes in nearly the same configuration as the original FABS. Comparison with the FABS data will be used to validate data from FABSI.

Monitor Diagnostics: The box labeled "total diag." receives 30% leakage through the telescope secondary. A diffuser at this location scatters light to several filtered diodes and 100 μm and 200 μm diameter optical fibers. These signals are available during the setup and testing phase for

system checkout. The signals will also be used to monitor FABSI operation.

Far-Field Diagnostics: Figure 2 is a schematic of the far-field imager gated optical imager (GOI). The phosphor output of a set of four S20 microchannel plate image intensifiers (MCPII) which can be

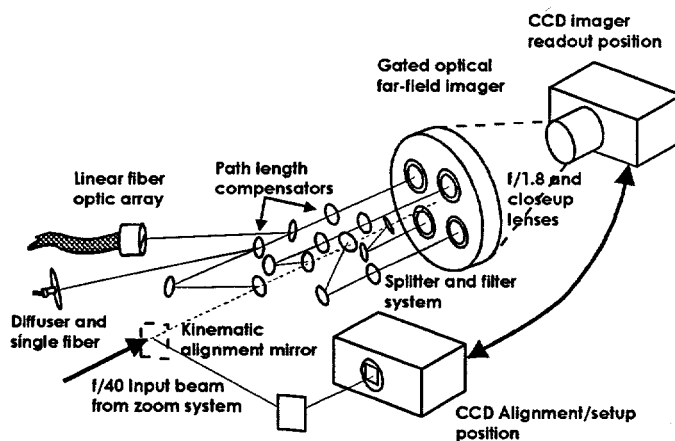


FIG. 2. Far-field imager.

gated as fast as 120 ps is lens coupled with a combination f/1.8 lens and close up lenses to a cooled 1024 X 1024 CCD array. There are about 250 CCD elements across each 18 mm MCPII. The MCPII has about 10 lp/mm resolution. The 20 μm FABSI optics resolution at the target translates to a 190 μm point spread at the MCPII photocathode. We have not yet measured the integrated system resolution but we do not expect the far-field imager to limit the system resolution.

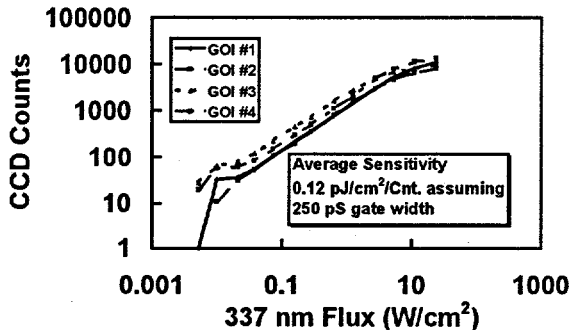


FIG. 3. Far-field imager sensitivity of four channels at full gain.

All detectors and imagers were calibrated for response vs. wavelength, time response, resolution where applicable and dynamic range. Figure 3 shows the MCPII/CCD response at full gain versus input flux from a N₂ laser at 337

nm. The MCPII was gated at 250 ps. The CCD/gated optical imager combination has a dynamic range of several hundred before it begins to lose resolution and saturate. The average full-gain imager sensitivity at 337 nm over the unsaturated range is 0.12 pJ/cm²/count assuming a nominal 250 ps gate. The CCD noise level for the readout rates and integration times typically used is ± 3 counts when operated at -35 deg. C.

The far-field imager beam splitter system in Fig. 2 is designed with near normal incidence Inconel splitters to minimize polarization effects. Additional flats are positioned in each leg where required to maintain identical optical path lengths from the splitter input to the photocathode on all four channels. Removal or addition of flats permits some variation of focus position at the target for individual channels. Some of the compensators are coated with Inconel so that each leg has identical transmission. One reflected image from the Inconel coated compensating flats is sampled by a single fiber. A second image is sampled by a 160 element linear fiber array. Step indexed (100 μm /110 μm /125 μm) 0.22 NA fused silica fiber was used. The linear array is available for streak recording or coupling to a spectrometer, but at this time, we have not completed a system. The single fiber is coupled through a splitter to two in-line filters; one for 351+10 nm band and one for 400 to 700 nm band. The two fibers are then coupled to the "2-color" streak camera to observe temporal correlation between the SRS and SBS at a single image point.

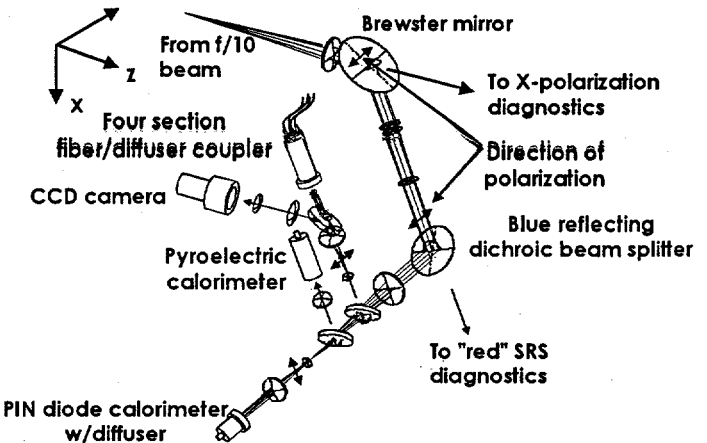


FIG. 4 "Y"-polarization SBS near-field diagnostics.

Different filters can be installed in front of each of the individual MCPIIs to permit imaging of SRS and SBS on the same shot.

Relative timing accuracy of the MCPII gates is <50 ps. For absolute timing, a 527 nm 100 ps optical fiducial pulse is injected into a four way optical fiber splitter. The optical pulse is imaged with GRIN lenses onto the edge of each MCPII. The MCPII which gates at zero time will record the

spot making it possible to absolutely time all the MCPII gates.

Figure 2 indicates the position of the kinematic mounted mirror and the cooled CCD which permits direct CCD imaging of alignment and resolution targets for optical adjustments. The CCD can integrate for several seconds and is therefore useful for imaging low level continuous light sources during setup.

Table I. Detector noise and sensitivities.

Detector	Signal	RMS Noise	Sens.
Near-field diag.			
CCD:	SBS	8 mV	0.42 V/J
	SRS	8 mV	74 V/J
PIN diode & dig.	SBS	0.2 mV	0.02 V/J
	SRS	0.2 mV	9 V/J
Pyro. Det.	SBS	50 μ V	1.5 μ V/J
	SRS	50 μ V	108 μ V/J
Far-field diag.			
CCD/GOI*	SBS	6 cnts	51 cnts/J
	SRS	6 cnts	

*Assumes 250 ps gate and 200 μ m diam source.

Near-field Diagnostics: Figure 4 shows a single leg of the near field diagnostics package. There are four identical sets; one each for the SRS and SBS bands and for each of two orthogonal polarizations. Uncoated Brewster angle wedges are used to select the polarizations. A 351 nm reflecting dichroic beam splitter and filtering then separates the blue from the red light. A dichroic beam splitter with two silicon PIN diodes receive the light that passes through the two Brewster mirrors.

The 12 ns FWHM PIN diodes shown in Fig. 4 are the primary calorimeter measurement. The 1 cm diameter diodes have a diffuser to insure spatially uniform response. The peak response of the diodes is linear to 10 V. The charge integrated signal is linear at least another factor of 50. The pyroelectric calorimeters were added for dynamic range and redundancy. The time integrated CCD cameras record the near-field images at the conversion crystal equivalent image plane.

Fused silica fibers with diffusers shown in Fig. 4 have been constructed however we do not have plans for recording these signals at this time.

Recording: Video signals are recorded on a variety of low resolution PC based digitizers and high resolution camac based digitizers. The far-field CCD has a 16-bit PC controlled digitizer. The diode signals are multiplexed with cable delays and recorded at 1 Gigasample/sec on four 8 bit Tektronics RTD720 digitizers.

The camac and high speed digitizers are PC controlled over GPIB interfaces. The pyroelectric detectors, which have a 1 ms time response are recorded on a slow, low noise, PC-based 12-bit digitizer. A variety of software is used to control

and read out the recorders. The computers can be controlled, and the data can be accessed by validated users over the internet.

Signal Levels: Table I gives the sensitivities to SRS and SBS backscatter of the various detectors in fractions of a Joule referenced at the target assuming minimum optical and electrical attenuation. Also given are the noise equivalent signals. The values are based on laboratory calibrations of the detectors and imagers and measurements of the optical components transmissions. The PIN diode noise levels is determined by the maximum single-bit sensitivity of the recording digitizer.

For comparison, a 2 mm diameter, 200 eV blackbody radiating for 10 ns would radiate ~ 0.4 mJ of visible light into the f/4.3 lens.

IV. SUMMARY

The diagnostics described here will provide a valuable capability in understanding the phenomena and source of backscatter associated with ICF experiments. The correlation of spatially resolved data obtained from the FABSI diagnostic with the existing spectral, calorimetric and angular distribution measurements will provide a clearer understanding of laser target-plasma interactions both in simple targets as well as the complicated indirect-drive hohlraum targets.

ACKNOWLEDGMENTS

The authors thank John Miller, John Moody, Brian MacGowan, Robert Kirkwood, Tim Weiland and Gregory Tietbohl of LLNL for information regarding the existing backscatter diagnostics, the Nova laser and for suggestions concerning FABSI.

¹R. L. Kauffman *et al.*, *LLNL ICF Quarterly Rep.* **5**, UCRL-LR-101582-95-4, 281 (1995).

²J. C. Fernández *et al.*, *Phys. Rev. E* **53**, 2747 (1996).

³D. H. Kalantar *et al.*, *Phys. Plasmas* **2**, 3161 (1995).

⁴

⁵H. A. Rose, and D. F. DuBois, *Phys. Fluids B* **5**, 590 (1993).

⁶B. MacGowan *et al.*, *LLNL ICF Quarterly Rep.* **5**, UCRL-LR-101582-95-4, 305 (1995).

⁷J. C. Fernández, R. R. Berggren, K. S. Bradley, W. W. Hsing, C. C. Gómez, J. A. Cobble, and M. D. Wilke, *Rev. Sci. Instrum.* **66**, 626 (1995).